Rev. Mexicana Astron. Astrof., 8, 155-161 (1983)

SPECTROSCOPIC OBSERVATIONS OF SUPERNOVA REMNANT CANDIDATES W28, CTB1, AND DR4

J. Bohigas

Instituto de Astronomía
Universidad Nacional Autónoma de México

M.T. Ruíz

Departamento de Astronomía
Universidad de Chile

L. Carrasco, L. Salas, and M.A. Herrera

Instituto de Astronomía
Universidad Nacional Autónoma de México

Received 1983 May 16

RESUMEN

Se presentan observaciones espectrofotográficas de W28, CTB1 y DR4 en la región espectral comprendida entre Hβ y la línea de azufre en λ6731 A. Se discuten las propiedades físicas de los candidatos a remanentes de supernova y se confirma que DR4, previamente identificado como la contraparte óptica del remanente en radio, es en realidad una región H II.

ABSTRACT

Spectrophotographic observations of W28, CTB1 and DR4 in the spectral range covering Hβ and the sulphur line at λ6731 A are presented. The physical properties of the supernova remnant candidates are discussed and it is verified that DR4, previously identified as the optical counterpart of the radio remnant, is actually an H II region.

Key Words: SUPERNOVAE REMNANTS – H II REGIONS

I. INTRODUCTION

The optical line ratios that separate supernova remnants (SNRs) from other objects are Hα/N II and, specially, Hα/S II. According to Sabbadin and D'Odorico (1976) these two ratios are typically less than 2.5 in galactic SNRs, though observations are typically less than 2.5 in galactic SNRs, though observations and theoretical models indicate that they may evolve towards slightly higher values as the remnant grows old (Daltabuit, D'Odorico, and Sabbadin 1976; Shull and McKee 1979; Bohigas 1983). This may lead to confuse a particular object –or parts of a particular object– as an SNR when its nature is quite another, specially when the inhomogeneities of the interstellar medium play a dominant role in its morphology and emission. In this paper we explore the nature of three SNR candidates (W28, CTB1 and DR4) which either seem to be relatively old or submerged in a particularly complex region or have been suspected to be H II regions. W28 is a remnant that is surrounded by molecular clouds and H II regions and, though its overall nature is firmly established, there are a few superimposed features that possess distinct characteristics and their status in relation to the SNR must be clearly established. CTB1 is apparently less complicated, though its morphology immediately suggests a medium that is mainly structured in the north-south direction. Furthermore, the remnant is thinly veiled by an H II region. Finally, van den Bergh, Marscher, and Terzian (1973) suggested that an emission nebula at the southern end of the radio remnant DR4 was part of the latter. This has been disqualified by radio observations and, to a lesser degree, by optical observations. In this paper we confirm the nature of this emission nebula as an H II region. In §2 we describe the observations and data reductions. In §3 we discuss our results and derive a few parameters for the confirmed remnants. Finally, §4 is devoted to the essential conclusions to which we are led.

II. OBSERVATIONS AND DATA REDUCTION

The spectra were obtained with the White spectrograph attached to the 84-inch telescope at the Kitt Peak National Observatory. The CIT image intensifier was used in combination with the Bowen Camera and grating No. 35. This set up yields a dispersion of 125 A mm^{-1}

with the blaze function peaked at 6750 A and a plate scale of 78.9 arcsec mm^{-1}. All the spectra were obtained with a slit whose dimensions were 2.93 mm long and 1.02 mm wide. Nitrogen baked IIIa-J plates were used. Plate characteristics were obtained from spot sensitometry performed in plates exposed and developed simultaneously. The spectra were digitized with the PDS 1050 model available at the Kitt Peak facilities in Tucson. The PDS slit was 5μm wide in the dispersion direction (covering 0.625 A) and 15μm long in the spatial direction (covering 1.18 arcsec). Averaging was carried out in both directions in order to increase signal-to-noise ratio, so that the spectral resolution was reduced by a factor of 2 and the spatial resolution by a factor of 3. Data reduction was carried out with a package of programs developed at the Instituto de Astronomía, UNAM.

Instrumental and atmospheric corrections were made with a theoretical function and crosschecked by comparing the derived line ratios for the planetary nebulae NGC 7662 and NGC 1535 with the mean values given by Kaler (1976) for these objects. Due to poor sky subtraction it was impossible to measure the faint lines characteristic of SNRs. In particular, the absence of the [O I] lines at λ6300 and λ6364 in Table 2, conspicuously bright in the night sky, is immediately apparent. On the other hand we used these two sky lines to determine the quality of the red end of our spectra (on theoretical grounds 6300/6364 = 3), and we estimate that the line ratios in this region of the spectrum are accurate within 25%. The quality of the blue end of the spectrum was investigated through the [O III] line ratio 5007/4959 (it should be equal to 3) and found that the line ratios within this region probably are 30% accurate, with the possible exception of CTB1 R2, where the signal is somewhat weaker.

Ratios involving lines from opposite ends of the spectrum depend on instrumental corrections, so that errors as large as 50% should not be surprising in this case. Finally, reddening corrections were made with the analytical formulae given by Miller and Mathews (1972) and assuming that Hα/Hβ = 3 in all cases. It is clear that Hα/Hβ will take this value only at a certain shock velocity, which in most theoretical shock wave models is approximately equal to 100 km s^{-1} (Dopita 1977; Raymond 1979; Shull and McKee 1979). This line ratio will increase with decreasing velocity and it can be as much as 23% larger for a shock velocity of 60 km s^{-1}. Thus the difference between the theoretical value and the one assumed here will always be less than the expected experimental errors, so that the assumption Hα/Hβ = 3 will only have a relatively minor effect.

Table 1 contains relevant data about our observations, such as the position at the slit center, the position angle (P.A.) and the exposure time. Figures 1, 2 and 4 (Plates) show the positions at which the spectra were taken (all plates are from van den Bergh *et al.* 1973). The spectroscopic results after reddening corrections are listed in Table 2. Finally, Table 3 includes the physical parameters derived for the two SNRs, W28 and CTB1.

TABLE 1

POSITIONS AND GENERAL DATA FOR THE OBSERVATIONS

Object	α (1950.0)	δ	Date	Exp. Time	P.A.
W28 R1	$17^h\ 57^m\ 31^s$	$-23°\ 12'.1$	17/9/77	$2^h\ 0^m$	110°
W28 R2	17 57 49	−23 27.4	18/9/77	1 30	170
CTB1 R1	23 58 07	61 56.2	16/9/77	2 0	56
CTB1 R2	23 55 22	61 58.0	17/9/77	2 0	134
DR4	20 20 38	40 03.2	16/9/77	1 30	50

III. DISCUSSION

Before discussing the spectral and dynamical properties of the observed objects, it is important to present the way in which the pre-shock densities are determined from the S^+ line ratio 6717/6731, which is readily observable in most SNRs. The density in the undisturbed medium is usually calculated by assuming that the compression in the cooling region is not limited by the magnetic field. This assumption is probably wrong in most cases (Cantó, private communication). From the momentum and mass conservation equations in the one dimensional case, and with the condition of a frozen-in magnetic field, it follows that

$$(\rho_1/\rho_0)^2\, V_{0A}^2 + (\rho_1/\rho_0)\,(V_{0A}^2 + C_0^2) - V_0^2 = 0, \qquad (1)$$

where ρ_1 and ρ_0 are the downstream and upstream mass densities, V_{0A} the upstream Alfvén speed defined as $(B_0^2/8\pi\rho_0)^{1/2}$, with B_0 being the interstellar magnetic field, C_0 is the upstream sound speed and V_0 is the shock velocity. In a medium where the magnetic field is 1 μG, the temperature is 10^4K, the particle number density is 1 cm^{-3} and the mass per particle is 2×10^{-24}g (leading to $C_0 \simeq 10$ km s^{-1} and $V_{0A} \simeq 1.4$ km s^{-1}, a compression factor (defined as ρ_1/ρ_0) of 35 would be sufficient so as to make magnetic pressure more important than thermal pressure. It is easy to see that thermal pressure alone can prevent a compression factor larger than 35 only if $V_0 \lesssim$ 45-50 km s^{-1}. Practically all SNRs have expansion velocities larger than this, indicating that the magnetic field plays a dominant role in the coolest region of the relaxation layer. For shock velocities larger than 70 km s^{-1} a convenient approximation to equation (1) is to disregard the thermal pressure, leading to the following equation

$$N_0 \simeq \left[\frac{N_e^2\, B_0^2}{8\pi m_p\, V_0^2}\right]^{1/3} \simeq 0.058 \left[\frac{N_e}{V_7}\right]^{2/3} \qquad (2)$$

where N_0 is the upstream number density, N_e is the electron density in the emitting region, m_p is the mass per particle and V_7 is the expansion velocity in units of 100 km s^{-1} The numerical value was calculated with the values of B_0 and m_p as stated above.

a) *W28*

Figure 1 (Plate) shows the positions at which this object was observed. On this photograph we have also drawn an incomplete and rather sketchy map of the main radio features superimposed or in the vicinity of the W28 SNR. The whole conglomerate, composed of H II regions, molecular clouds and the SNR itself, occupies a square degree area of the sky (Goudis 1976). The most prominent members of the conglomerate are the Trifid nebula and the remnant, which fills a circle with a diameter not larger than 45′. There is some uncertainty as to whether all these components are physically connected or not, mainly because of the wide range of possible distances to the remnant and the H II regions. On the other hand Pastchenko and Slysh (1974) detected a molecular cloud from OH absorption observations and concluded, from the large velocity dispersion in the cloud, that the SNR and this object are physically related. This OH cloud forms an arc surrounding the western edge of W28, and it is shown in Figure 1 (Plate). Wootten (1981) studied the region at millimetric wavelengths hoping to detect some evidence indicating that a star formation process in under way, as seems to be the case in W44 (Wootten 1977). No such thing was observed in W28. Instead, he discovered a dense molecular cloud situated perpendicularly to the OH arc (see Figure 1-Plate) that seems to be interacting in some way with the SNR. In particular, he believes that the broad HCO^+ lines originate from a region of enhanced ionization produced by the penetration of energetic radiation from W28. The absence of an embedded infrared source supports this idea. DeNoyer (1983) is also inclined to this conclusion on the basis of similar features in HCN and CS. Radio observations have also disclosed the presence of other possible H II regions besides the Trifid nebula, such as G5.9–0.4, KE59 and G6.4–0.5. Yet, Goudis (1976) is a bit wary about identifying unambiguously the last two sources as H II regions, suggesting that more observational work is necessary in order to arrive to a firmer conclusion. In summary, long wavelength observations of the region indicate that it is composed of a number of different objects at or near the position of the remnant and, in some cases, interacting with it. Thus, we might expect a complex physical and velocity structure of the W28 SNR, with two possible qualitative features in the optical spectrum; contamination from H II regions adjacent or superimposed to the remnant and, maybe, some variation in the extinction values.

In order to explore the nature of the two suspected internal H II regions we obtained the spectrum of G6.4–0.5, which corresponds to object W28 R2 in Table 2. This object is characterized by a radio spectrum with a spectral index of –0.21, very close to the mean value of –0.28 found in 'plerion'type SNRs (Caswell 1979), and no radio recombination lines. Thus, it was not clear if this object is indeed an H II region or not. We believe

TABLE 2

RELATIVE LINE INTENSITIES OF THE OBSERVED OBJECTS[a]

Object	Size (arcsec)	5007/Hβ	Hα/N II	Hα/S II	6717/6731	Ne (cm^{-3})
W28 R1–1	57	0.28(0.07)	1.44(0.11)	1.56(0.19)	1.35(0.16)	110
–2	11	0.68(0.03)	1.28(0.11)	1.32(0.09)	1.23(0.07)	275
–3	106	0.42(0.16)	1.44(0.12)	1.59(0.34)	1.36(0.15)	100
W28 R2	145	0.47(0.14)	1.75(0.39)	3.96(0.90)	1.19(0.25)	330
CTB1 R1–1	78	0.72(0.27)	1.90(0.29)	1.75(0.32)	1.44(0.12)	10
–2	25	1.58(0.29)	2.63(0.45)	2.73(0.37)	1.33(0.14)	130
–3	92	0.59(0.15)	1.87(0.23)	1.88(0.41)	1.12(0.26)	480
CTB1 R2–1	92		2.14(0.35)	1.46(0.23)	1.43(0.28)	10
–2	39	1.72(0.25)	2.70(0.50)	2.01(0.37)	1.19(0.18)	330
–3	53		2.56(0.31)	1.50(0.22)	1.25(0.15)	240
DR4–1	64	0.62(0.10)	2.00(0.45)	5.18(1.69)	1.30(0.25)	125
–2	74	1.36(0.25)	3.14(0.29)	7.54(0.80)	1.38(0.15)	75
–3	99	0.58(0.22)	2.26(0.33)	5.56(1.20)	1.44(0.21)	10

a. The relative line intensities are for Hα = 3 and Hβ = 1. N II represents the sum of the relative intensities of the N^+ lines at 6548, 6584 A, and S II the sum of the S^+ lines at 6717, 6731 A. The standard deviation for each quantity is in parenthesis.

that the relative line intensities conclusively show that W28 R2 is strongly contaminated by an H II region, if it is not one. The mean electron density determined from our observations is equal to 330 cm^{-3}, very similar to the value derived from radio observations. Finally the mean extinction for the region is $\langle E_{B-V} \rangle = 1.23$, with a standard deviation σ of 0.39.

The spectrum of W28 R1 has been separated in three components since W28 R1–2 seems to be qualitatively different to the other two regions, a difference that is emphasized by the stronger relative intensity of the [O III] 5007A line in this region. Nevertheless, the three spectra are characteristic of SNRs. Yet, none of them is similar to the two spectra presented by Dopita, Mathewson, and Ford (1977), in which the nitrogen and sulphur lines are, for such an apparently evolved object, uncharacteristically strong. It is difficult to make an assessment of these differences, since Dopita *et al.* provide no information as to the positions of the observed regions. Though our observations contain a relatively small number of lines, these are the most important in SNRs, and a comparison with theoretical models is by no means useless. The relative intensity of the [O III] line at 5007 A with respect to Hβ indicates that the shock velocity is between 60 and 90 km s^{-1} (Raymond 1979; Shull and McKee 1979, RA and SM hereafter). No theoretical model is capable of reproducing our results, though an interpolation between models C and D of SM seems to be the best alternative, especially for region W28 R1-2. This leads to a shock velocity of approximately 85 km s^{-1} if the ambient medium has a density of 10 cm^{-3}, a magnetic field of 1 μG and cosmic composition. On the other hand, interferometric observations by Lozinskaya (1980) yielded a mean expansion velocity of 40 km s^{-1}. though individual filaments moving at velocities of 60 to 80 km s^{-1} suggest, as these observations do, a higher expansion velocity than this mean value. Furthermore, if the velocity dispersion of 50 km s^{-1} found by Pastchenko and Slysh (1974) is produced by the interaction with the remnant, then the expansion velocity in the northeastern region where W28 R1 is situated, where no cloud complex has so far been detected, must be above the mean value. In any case, a kinematical study of W28 must consider the density structure of the medium and a model such as the one produced by Kompaneets (1960) should be used, as has already been done in IC443 (Lozinskaya 1979) and G65.3 + 5.7 (Rosado 1981). Consequently, the pre-shock density in the three regions of W28 R1 have been calculated with equation (2) and assuming that the expansion velocity is equal to 80 km s^{-1}. All three regions point to a pre-shock density approximately equal to 2 cm^{-3}. Since the ram pressure (ρV^2) along the shock is approximately constant, we can estimate the expansion velocity of the remnant as it moves into the molecular clouds if their density is known. In the OH cloud, where $N \tilde{=} 25$ cm^{-3}, we find an expansion velocity approximately equal to 25 km s^{-1}, a factor of 2 smaller than the velocity dispersion found by Pastchenko and Slysh (1974), but identical to the line-width found by Goss (1968) in OH absorption. For the CO cloud the density is roughly equal to 2.5×10^3 cm^{-3}, which leads to an estimated expansion velocity in the cloud of 2.3 km s^{-1}, almost identical to the 2 km s^{-1} expansion velocity reported by Wootten (1981). Thus, the kinematic results of these three different regions into which the W28 SNR is expanding seem to be fairly consistent.

The distance to W28 has been calculated using a variety of methods (OH, 21-cm and HCOH absorption, kinematics and the Σ–d relation), leading to results in the range of 1.2 to 3 kpc (Goudis 1976; Clark and Caswell 1976), with the mean value being equal to 2.2 kpc. From our spectrum we derive $E_{B-V} = 1.16$ ($\sigma = 0.39$), which would be consistent with a distance of 2 kpc, if

TABLE 3

PHYSICAL PARAMETERS OF SNRs W28 AND CTB1

	Distance (kpc)	Diameter (arcmin)	V_7 (100 km s^{-1})	N_0 [a] (cm^{-3})	E_{50} [a] (10^{50} erg)	t_4 (10^4 year)
W28 R1–1	2.0	45	0.8	1.56	1.2	5.0
–2				2.86	2.4	
–3				1.46	1.1	
CTB1 R1–1	4.5	30	0.9	0.29	0.9	6.8
–2				1.60	5.2	
–3				3.81	12.4	
CTB1 R2–1	4.5	30	0.9	0.31	1.0	6.8
–2				2.97	9.7	
–3				2.40	7.8	

a. The pre-shock densities and energies derived from CTB1 R1–1 and CTB1 R2–1 are probably different to the real values (see text).

the extinction is equal to the mean value of 0.61 mag kpc^{-1} given by Spitzer (1978). It is worth noticing that similar extinction values are found for W28 R2, suggesting that the W28 SNR and the H II region G6.4–0.5 are not only superimposed, but actually share the same region in space, a region characterized by an extreme complexity.

To estimate the energy deposited in the ejected mass by the supernova explosion we must first assess the evolutionary stage at which W28 is at the present time. If the expansion velocity, as determined from the optical spectrum, is close to the maximum value, then there is no doubt that the object has been in the radiative phase for some time. Furthermore, the pre-shock density we have just calculated indicates that no cloud collision is producing the optical emission, suggesting that the estimated expansion velocity is indeed close to its maximum. On the other hand there are no X-ray observations capable of revealing the presence of faster components in the remnant. Thus, we assume that W28 is in the radiative phase and calculate its age and energy from Chevalier's (1974) model. This leads to expressions:

$$E_{50} = 3.3 \times 10^{-4}\, N_0^{1.12}\, V_7^{1.4}\, R_{pc}^{3.12}\,, \qquad (3)$$

$$t_4 = 0.304\, R_{pc}/V_7\,, \qquad (4)$$

where E_{50} is the initial energy in units of 10^{50} erg, R_{pc} is the shock radius in units of parsec and t_4 is the age of the SNR in units of 10^4 year. If we combine equations (2) and (3) we find that $E \propto V^{0.6}\, R^{3.12}$ which shows that energy estimates will depend almost exclusively on the assumed distance to the object, since the velocity dependence is comparatively negligible. The results are given in Table 3 and we find an energy roughly equal to 2×10^{50} erg for the parameters chosen, suggesting a Type I supernova progenitor for W28.

b) *CTB1*

Figure 2 (Plate) shows the positions at which the observations were carried out on CTB1. Optical emission is concentrated in a thin cusp on the southern half of the remnant. High resolution radio maps at 49 and 21-cm show that the optical component has a coincident radio counterpart (Dickel and Willis 1980), as has been observed in most old SNRs with the exception of Puppis. According to Duin and van der Laan (1975) this behavior can be explained if the intense radio emission is also produced by the thermal compression of the shocked gas, that drags the magnetic field and relativistic particles along. At the western peak of radio emission no optical emission has so far been detected, whereas the north-eastern region is conspicuously faint in both radio and optical frequencies. According to Willis and Dickel (1971) the SNR is embedded in a large faint H II region. These authors also point out the presence of a neutral hydrogen cloud in the vicinity of CTB1, and there seems to be some evidence indicating an interaction between the cloud and the SNR (Dickel and Willis 1980). No high quality X-ray observations have yet been made, and only upper limits to the X-ray flux are reported by Gronenschild (1979).

The morphology or the medium surrounding CTB1 cannot be established precisely. Yet a few qualitative statements can be made about it. Following Duin and van der Laan (1975) the volume emissivity in the compressed region is given by

$$\epsilon = \epsilon_0\, (n/n_0)^{(\gamma+1)/2}\, (B/B_0)^{\gamma+1} \qquad (5)$$

where ϵ_0 is the interstellar value and $\gamma = 1 + 2\alpha$ ($\alpha > 0$ is the spectral index). Assuming a frozen-in field it follows that $(n/n_0)_{west} > (n/n_0)_{south}$, since radio emission is stronger on the western side. On the other hand, the optical emission in the west is so far invisible. There are three possible reasons:

(a) large extinction along the western ridge, a possibility that is questionable only from star counts,

(b) the shocked gas has already cooled down below the characteristic optical temperatures, or

(c) the optical emissivity is small because $n_{west} < n_{south}$.

Assuming that the third possibility is correct, it follows that the interstellar medium is denser in the southern edge of CTB1. Similarly, since the ram pressure along the shock is roughly constant, is follows that the shock velocity is larger on the western side. Finally, if equation (2) is valid, it follows that the magnetic field on the western region is also larger, precluding in this way a higher compression factor and, consequently, higher optical emission.

The line ratios derived from the optical spectrum of the two regions of CTB1 are given in Table 2. Each region has been separated in three zones according to the criterion previously described for W28. A scan of the relative fluxes is presented in Figure 3. These regions have been studied previously by D'Odorico and Sabbadin (1977). Our reported values for Hα/N II and Hα/S II are 60% larger than theirs. Although the regions here studied are apparently coincident with regions 7,8 and 1,2,3,4 observed by these authors, direct comparison of the two sets of data is difficult as their published coordinates suffer a displacement in right ascension with respect to the true position of the SNR filaments. Our derived line ratios Hα/N II and Hα/S II are somewhat larger than what is considered to be normal, though still within the limits defined by SNRs. This is an unlikely effect due to poor sky subtraction, since in a "normal" night at Kitt Peak the Hα intensity is not more than 10% of that of [O I]λ6300, whereas in our spectra the former is 1-1.5 times more intense. There are some possible explanations as to why these line ratios appear

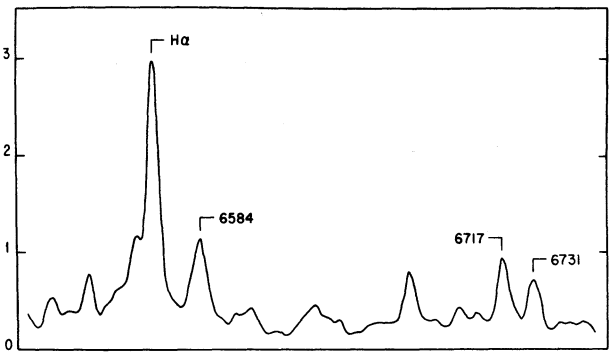

Fig. 3. Typical scan on the spectrum of CTB1 R1–3. Notice the high relative intensity of Hα with respect to the sulphur lines and, specially, the nitrogen lines. The scale is arbitrary.

to be so large. First, they might occur if the observed regions are not dominated by low ionization species. Indeed, the relative line intensities in CTB1 R1 and CTB1 R2 indicate that the [O III] line at 5007 A is stronger where Hα/N II and Hα/S II are larger. Secondly, there is an undetermined contribution from the H II region veiling CTB1 which would tend to increase both line ratios. Finally, the nitrogen abundance gradient in our galaxy, which is also apparent from SNRs (González 1983), would also lead to a larger than normal value for Hα/N II in CTB1 since this object is at an estimated galactrocentric distance of 12.8 kpc (Ilovaisky and Lequeux 1972; Clark and Caswell 1976). At this distance nitrogen is 1.2 times less abundant than the usual cosmic value, and consequently, the value of Hα/N II will be consistently 1.2 times larger than what is considered normal.

Again, none of the existing theoretical models can reproduce quantitatively our results, though all of them preclude shock velocities larger than 90 km s^{-1} on the basis of the relative intensity of the [O III] line at 5007 A. There is an important qualitative difference between the predictions of RA and those of SM. In all cosmic composition models the former predicts that Hα/N II > Hα/S II, whereas the opposite is true in the models of SM, in our observations and in those of D'Odorico and Sabbadin (1977). The only models in which RA can account for this aspect of the spectrum are those with a depleted cosmic composition and a shock velocity of 70.7 km s^{-1} (models BB and HH). As a matter of fact, model BB is reasonably close to the spectrum of CTB1 R1–2 and CTB1 R2–2, though the Hα/S II ratio is underestimated. But, as with W28, in all cases the best alternative is again an interpolation between models C and D of SM, suggesting a shock velocity of approximately 85 km s^{-1}. On the other hand, interferometric observations by Lozinskaya (1980) point to higher values for the shock velocity, probably between 150-200 km s^{-1}, but with a rather large number of features expanding at considerably smaller velocities. We believe that the constraint put forward by the relative intensity of the 5007 A line is quite strong, indicating that the shock velocity in the observed regions cannot be much larger than 90 km s^{-1}. Consequently we selected this value when computing the pre-shock density and the energy. The pre-shock densities obtained for CTB1 R1–1 and CTB1 R2–1 indicate that either the shock is very weak in these regions, precluding larger compression factors, or the preshock density is comparatively small.

There is some uncertainty as to the distance to CTB1. The Σ–d relation leads to distance in the range of 4.7 to 5.8 kpc (Ilovaisky and Lequeux 1972; Clark and Caswell 1976; Dickel and Willis 1980). But on the basis of suspected associations with OH clouds and kinematic estimates a much smaller distance of 2.1 to 2.8 kpc has been suggested by Dickel and Willis (1980). The discrepancy might be due to the statistical nature of the Σ–d relation, so that when applied to an individual object it can lead to a distance that is substantially different to the real value. Optical spectra would help to clarify this situation if the mean absorption coefficient in the direction of CTB1 was well known. In CTB1 R1 we find $\langle E_{B-V} \rangle = 0.56$ ($\sigma = 0.20$); whereas in CTB1 R2, where the signal is weaker, we find a very uncertain $\langle E_{B-V} \rangle = 0.13$ ($\sigma = 0.10$). The CGO catalogue (Cruz-González *et al.* 1974) reports two stars in the vicinity of CTB1, CGO661 and CGO662, whose reddening is very similar to that of CTB1 R1 (0.60 and 0.59 respectively) but each one situated at a substantially different distance to the Sun (4.6 and 2.8 kpc), suggesting an extreme patchiness in the medium contained between us and the remnant. In the understanding that any choice regarding the distance to the object is uncertain, we will assume that CTB1 is 4.5 kpc away from the Sun. Formulae (3) and (4) are used to calculate the age and energy of the SNR.

The energies derived for CTB1 R1–1 and CTB1 R2–1 are roughly 10 times less than those obtained from the other regions. It is difficult to establish the precise origin of this discrepancy, since the sulphur line ratio from where the preshock density is obtained is in the low density region, where any small variation in 6717/6731 leads to vast differences in the density. Yet, it seems reasonable to assume that the shock velocity in CTB1 R1–1 and CTB1 R2–1 is larger than assumed here, which would lead to a smaller pre-shock density but also a larger energy (since $E \propto V^{0.6}$). The other four regions lead to a mean energy of 9×10^{50} erg, which is very similar to the energy that Cygnus, a morphologically similar remnant (van den Bergh *et al.* 1973), is supposed to have. Yet, Cygnus is obviously a younger remnant than CTB1, with an important part of it still moving in the adiabatic expansion phase.

c) *DR4*

Figure 4 (Plate) shows the positions at which this object was observed. The optical nebulosity identified

by van den Bergh *et al.* (1973) as corresponding to the synchrotron radio source classified as an SNR has been disputed as such by a number of authors (Higgs, Landecker, and Roger 1977; Baars, Dickel, and Wendker 1978). Working at radio frequencies and higher resolution, they disclosed the presence of an H II region embedded in the remnant's radio emission and coincident with the optical nebulosity identified by van den Bergh *et al.* Optical observations carried out by D'Odorico and Sabbadin (1977) also showed that the emission from the optical nebula that van den Bergh *et al.* associated to the remnant is heavily contaminated by an H II region, if not totally dominated by it. Our observations, with the slit position angle situated perpendicularly to theirs, show even more conclusively that the object is an H II region.

IV. CONCLUSIONS

The observed spectra and the preceding discussion lead to the following essential conclusions:

1. The spectrum of W28 R2 supports the proposal that G6.4–0.5 is an H II region (Goudis 1976). Furthermore, the similar extinction values found for the W28 SNR and this H II region indicate that both objects occupy the same space.

2. The total energy of W28 suggests a Type I supernova progenitor for this object. A kinematical treatment based on Kompaneets (1960) work is suggested on the basis of the highly inhomogeneous nature of the medium surrounding the SNR.

3. The CTB1 SNR seems to be energetically similar to Cygnus, but substantially older. At present it is impossible to make a quantitative assessment on the physical parameters of the surrounding medium, though it seems probable that the pre-shock density is smaller in the western than in the southern region, whereas the opposite is true for the shock velocity and upstream magnetic field.

4. Finally, the models of Shull and McKee (1979) give better results than those of Raymond (1979). This should not be surprising, since at shock velocities smaller than 100 km s^{-1} the ionization state of the surrounding medium, produced by the radiation emitted from the relaxation region behind the shock front, is strongly dependent on the velocity. Consequently, a self-consistent solution must be much more appropriate.

This is Contribution No. 113 of Instituto de Astronomía, UNAM.

REFERENCES

Baars, J.W.M., Dickel, H.R., and Wendker, H.J. 1978, *Astr. and Ap.*, **62**, 13.
Bohigas, J. 1983, *Rev. Mexicana Astron. Astrof.*, **5**, 271.
Caswell, J.L. 1979, *M.N.R.A.S.*, **187**, 431.
Clark, D.H. and Caswell, J.L. 1976, *M.N.R.A.S.*, **174**, 267.
Chevalier, R.A. 1974, *Ap. J.*, **188**, 501.
Cruz-González, C., Recillas-Cruz, E., Costero, R., Peimbert, M., and Torres-Peimbert, S. 1974, *Rev. Mexicana Astron. Astrof.*, **1**, 211.
Daltabuit, E., D'Odorico, S. and Sabbadin, F. 1976, *Astr. and Ap.*, **49**, 119.
De Noyer, L.K. 1983, *Ap. J.*, **264**, 141.
Dickel, J.R. and Willis, A.G. 1980, *Astr. and Ap.*, **85**, 55.
D'Odorico, S. and Sabbadin, F. 1977, *Astr. and Ap. Suppl.*, **28**, 439.
Dopita, M.A. 1977, *Ap. J. Suppl.*, **33**, 437.
Dopita, M.A., Mathewson, D.S. and Ford, V.L. 1977, *Ap. J.*, **214**, 179.
Duin, R.M. and van der Laan, H. 1975, *Astr. and Ap.*, **40**, 111.
González, J. 1983, *Rev. Mexicana Astron. Astrof.*, **5**, 289.
Goss, W.M. 1968, *Ap. J. Suppl.*, **15**, 131.
Goudis, C. 1976, *Ap. and Space Sci.*, **40**, 91.
Gronenschild, E.H.B.M. 1979, *Astr. and Ap.*, **77**, 53.
Higgs, L.A., Landecker, T.L. and Roger, R.S. 1977, *A.J.* **82**, 718.
Ilovaisky, S.A. and Lequeux, J. 1972, *Astr. and Ap.*, **18**, 169.
Kaler, J.B. 1976, *Ap. J. Suppl.*, **31**, 517.
Kompaneets, A.S. 1960, *Sov. Phys. Doklady*, **5**, 46.
Lozinskaya, T.A. 1979, *Astr. and Ap.*, **71**, 29.
Lozinskaya, T.A. 1980, *Astr. and Ap.*, **84**, 26.
Miller, J.S. and Mathews, W.G. 1972, *Ap. J.*, **172**, 591.
Pastchenko, M.I. and Slysh, V.I. 1974, *Astr. and Ap.*, **35**, 153.
Raymond, J.C. 1979, *Ap. J. Suppl.*, **39**, 1.
Rosado, M. 1981, *Ap. J.*, **250**, 222.
Sabbadin, F. and D'Odorico, S. 1976, *Astr. and Ap.*, **49**, 119.
Shull, J.M. and McKee, C.F. 1979, *Ap. J.*, **227**, 131.
Spitzer, L. 1978 in *Physical Processess in the Interstellar Medium* (New York: John Wiley and Sons).
van den Bergh, S., Marscher, A.P. and Terzian, Y. 1973, *Ap. J. Suppl.*, **26**, 19.
Willis, A.G. and Dickel, J.R. 1971, *Ap. Letters*, 8, 203.
Wootten, H.A. 1977, *Ap. J.*, **216**, 440.
Wootten, H.A. 1981, *Ap. J.*, **245**, 105.

Joaquín Bohigas, Luis Carrasco, Miguel Angel Herrera and Luis Salas: Instituto de Astronomía, UNAM, Apartado Postal 70-264, 04510 México, D.F., México.
Ma. Teresa Ruíz: Universidad de Chile, Departamento de Astronomía Casilla 36-D, Santiago de Chile.

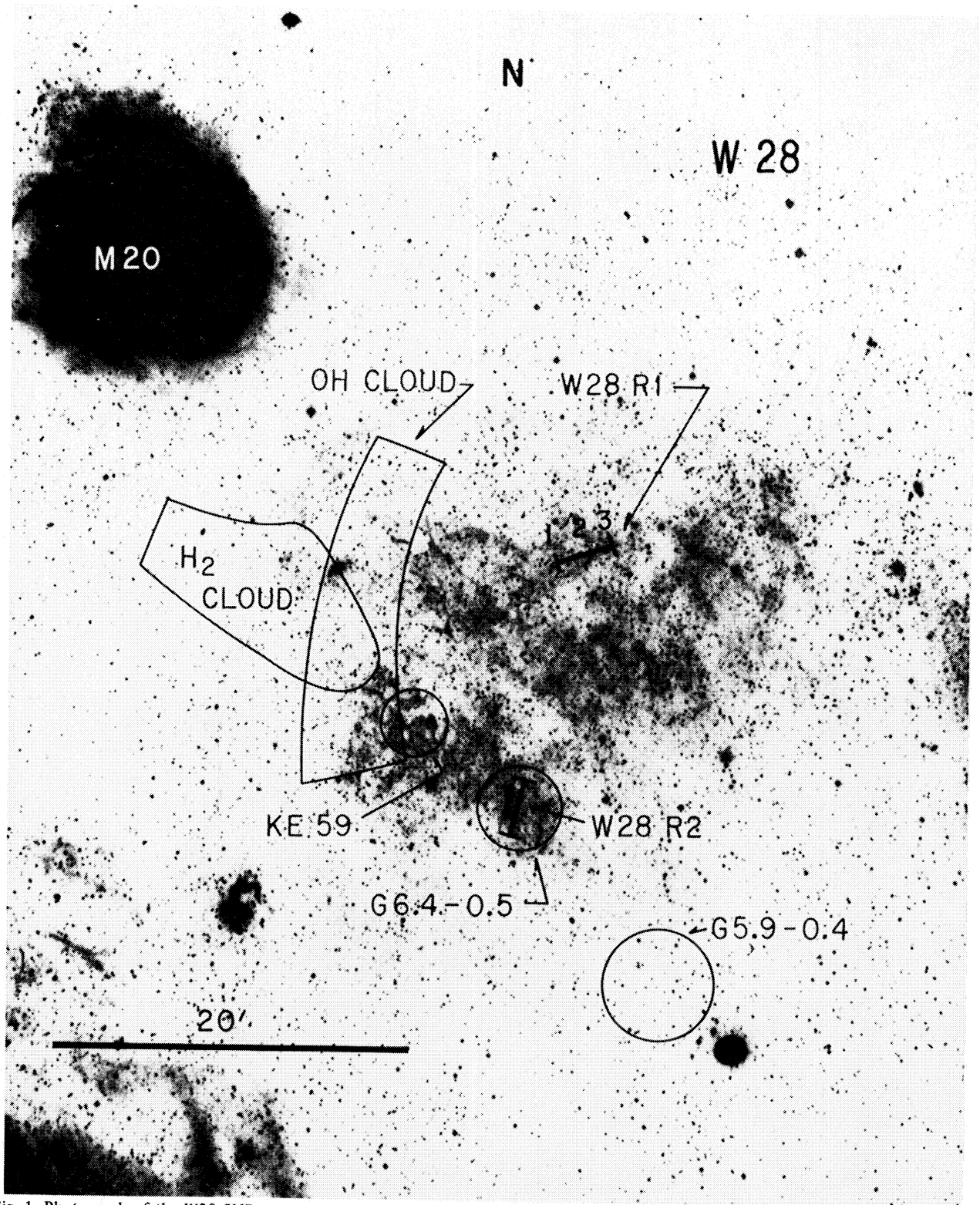

Fig. 1. Photograph of the W28 SNR and map of several other features in the region. The positions at which the spectra were taken are W28 R1 and W28 R2.

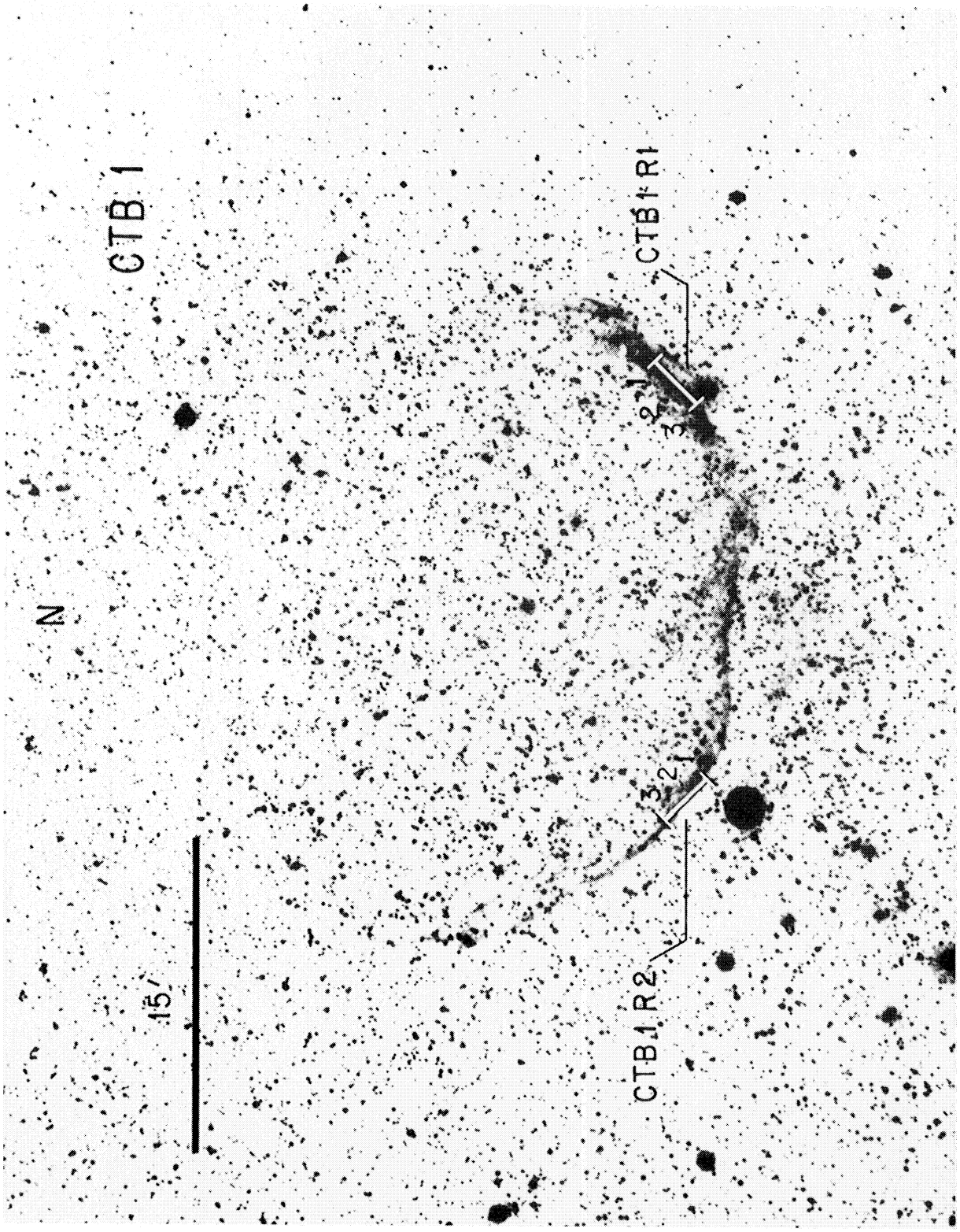

Fig. 2. Photograph of the CTB1 SNR. The object was observed at positions CTB1 R1 and CTB1 R2.

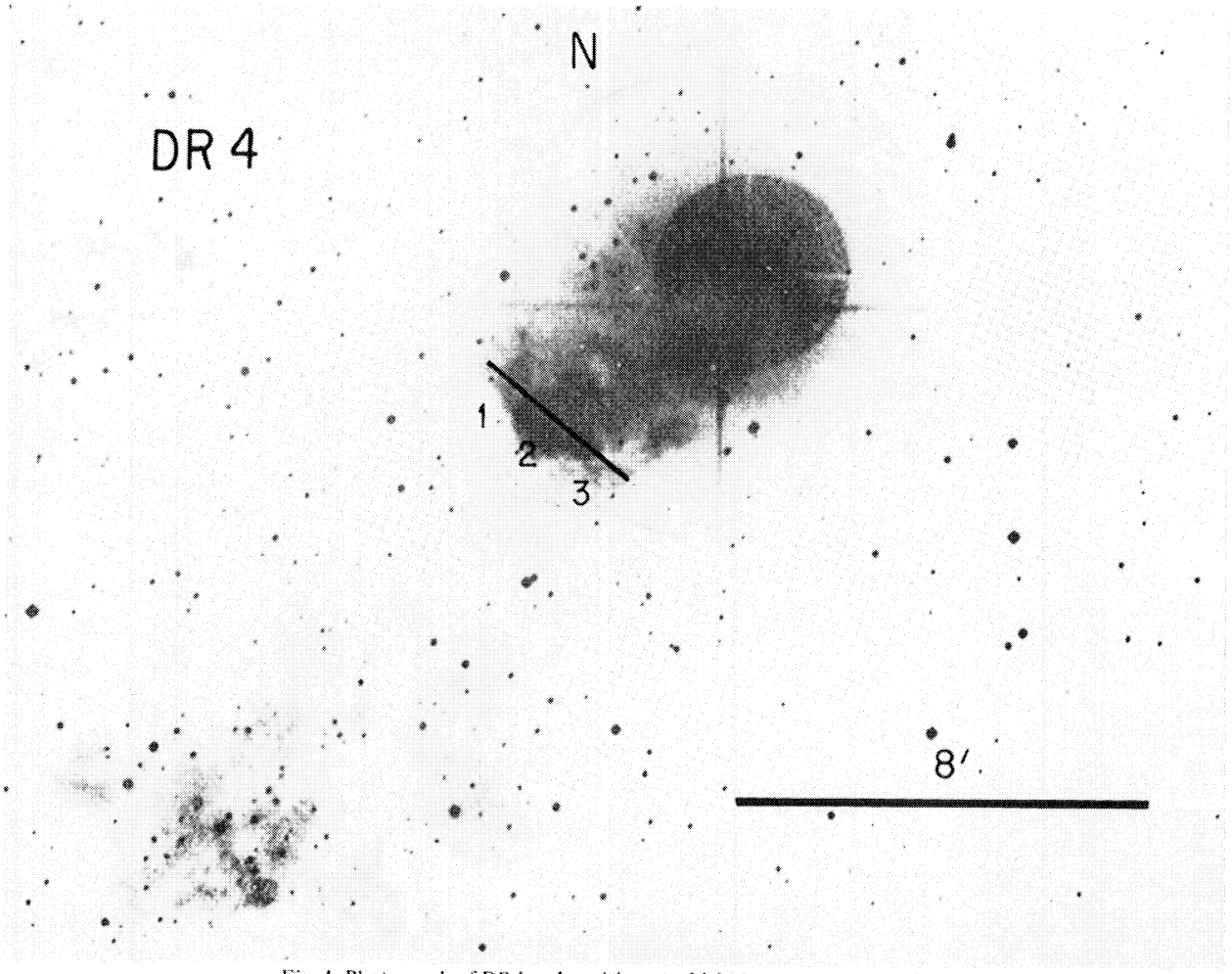

Fig. 4. Photograph of DR4 and position at which the spectrum was taken.